

Simulating the initial growth of a deposit from colloidal suspensions

T. J. Oliveira¹ and F. D. A. Araújo Reis²

¹ Departamento de Física, Universidade Federal de Viçosa, 36570-900, Viçosa, MG, Brazil

² Instituto de Física, Universidade Federal Fluminense, Avenida Litorânea s/n, 24210-340 Niterói, RJ, Brazil

E-mail: tiago@ufv.br, reis@if.uff.br

Abstract.

We study the short time properties of a two-dimensional film growth model in which incident particles execute advective-diffusive motion with a vertical step followed by D horizontal steps. The model represents some features of the deposition of anisotropic colloidal particles of the experiment in Phys. Rev. Lett. **110**, 035501 (2013), in which wandering particles are attracted to particle-rich regions in the deposit. Height profiles changing from rough to columnar structure are observed as D increases from 0 (ballistic deposition) to 8, with striking similarity to the experimental ones. The effective growth exponents matches the experimental estimates and the scaling of those exponents on D show a remarkable effect of the range of the particle-deposit interaction. The nearly ellipsoidal shape of colloidal particles is represented for the calculation of roughness exponents in conditions that parallel the experimental ones, giving a range of estimates that also include the experimental values. The effective dynamic exponents calculated from the autocorrelation function are shown to be suitable to decide between a true dynamic scaling or transient behavior, particularly because the latter leads to deviations in an exponent relation. These results are consistent with arguments on short time unstable (columnar) growth of Phys. Rev. Lett **111**, 209601 (2013), indicating that critical quenched KPZ dynamics does not explain that colloidal particle deposition problem.

1. Introduction

The scaling properties of growing interfaces attracted much interest in the last decades due to the large number of problems of technological and fundamental interest in which the physical and chemical properties are affected by interface morphology [1, 2]. This scenario motivated the proposal of models based on stochastic equations, which represent the main symmetries of the growth processes and define universality classes, and the development of atomistic models that capture the details of those processes and are frequently suitable for particular applications. Among the hydrodynamic models, the Kardar-Parisi-Zhang (KPZ) equation [3] deserves special interest due to the large number of possible applications and the recent progress in its solution [4, 5, 6, 7].

However, there are frequent debates on the universality class of growth processes in which different scaling exponents are measured when the growth conditions are changed (e. g. changes in temperature, reactant flux, or electric potential) [8, 9, 10, 11, 12, 13, 14]. Several stochastic equations and atomistic models actually show variations of scaling exponents as the growth conditions change. In many cases, these features are related to crossovers between different dominant dynamics at different time and length scales [15, 16, 17, 18, 19, 20, 21]. Many of those models show crossover to KPZ scaling.

In a recent work, Yunker et al. [22] studied the deposition of colloidal particles in the water-air interface of evaporating drops, showing that scaling exponents of height fluctuations and the height distributions changed with the aspect ratio ϵ of the particles. As ϵ increased, those changes were explained as transitions from uncorrelated (Poisson-like) deposition to normal KPZ scaling and then to critical KPZ scaling with quenched disorder (QKPZ) [23] in $1 + 1$ dimensions. The main physical change in the system as ϵ increases seemed to be the onset of a kind of “Matthew effect” [24], in which wandering particles are attracted to rich-particle regions in deposit. It explains the transition from Poisson to ballistic (KPZ) growth when the particle shape changes from spherical (no interaction) to slightly elliptical (small attraction). However, Nicoli et al. [25] showed that a morphological instability (and consequent anomalous roughening) may be the origin of those exponent changes, so that the claim of QKPZ scaling is not necessary (although Yunker et al. [26] argue that the initial roughness of the contact line may be the source of that disorder).

This scenario motivates the present study of a deposition model of diffusing particles with a drift, which is an extension of a model proposed by Rodríguez-Pérez, Castillo and Antoranz [27], hereafter called RCA model. In this model, the mechanisms of particle advection and diffusion before aggregation is consistent with the above mentioned experiment for large ϵ [22], since the diffusive flow leads to preferential sticking at prominent regions of the deposit. The growth of large and thick deposits with the RCA model showed that it is in the KPZ class in $2 + 1$ dimensions [27, 28], and here we show that the extended model is also in that class in $1 + 1$ dimensions. However, the main interest of the present work is to study the scaling of height fluctuations of deposits with small average thicknesses, of the same order of magnitude of the thicknesses of colloidal

particle deposits of Ref. [22]. The effect of particle shape on the surface morphology is analyzed using the intra-grain modeling of Ref. [29].

For small values of the advection-to-diffusion rate (Peclet number), our model provides interface profiles with columnar structures at short times, which leads to estimates of (effective) growth exponents that significantly exceed both the KPZ and the uncorrelated deposition values ($1/3$ and $1/2$). After representing the ellipsoidal particle shapes at the surface, the local roughness exponent attains large values in nearly two decades of window size. The interface profiles are similar to the colloidal particle deposits of Ref. [22], for average heights of the same order, and several values of effective exponents are in the ranges reported in that work. Scaling arguments explain the dependence of the growth exponent on the lateral diffusion coefficient of the model, showing that small changes in the range of attraction to the deposit may lead to significant changes in that exponent. Thus, a description of that experiment without accounting for critical disorder mechanisms seems to be possible, in agreement with Ref. [25]. The study of the scaling of the zeros and minima of the autocorrelation function is proposed as an additional test for the universality class in these problems. Our model is also shown to have asymptotic KPZ scaling, which raises the possibility that the colloidal particle deposition is also in the KPZ class for any $\epsilon > 1$, but with strong scaling corrections.

The rest of this work is organized as follows. In Sec. 2 the deposition model is presented in detail as well as the definition of all quantities analyzed in this work. Sec. 3 shows results for deposits and height profiles and discuss the variation in the growth exponents. In Sections 4 and 5, results for dynamic and local roughness exponents are shown, respectively. In Sec. 6, we provide numerical evidence that the model is asymptotically in the KPZ class. Our final conclusions are presented in Sec. 7.

2. Model, simulation and quantities of interest

The model is defined in a square lattice with an initial planar substrate at $y = 0$. Each site may be empty or occupied by a particle of linear size d . Each deposition step begins with a new particle being left at a random position above the deposit. This particle executes steps in a ballistic-diffusive sequence, which consists of one vertical down step followed by D horizontal random steps. When this particle reaches a site with a nearest neighbor occupied site or a substrate site, it permanently aggregates there. The time unity is defined as the time of deposition of L particles.

This model is slightly different from the RCA model because the latter allows the random steps to be performed in the horizontal or in the vertical direction. For more details on the physico-chemical motivation of the RCA model, we suggest the reader to consult Ref. [27]. Similar models with multiparticle flux were proposed in Refs. [30, 31] and a recent extension in Ref. [32].

Diffusion-limited aggregation (DLA) [33] is a widely used model for electrochemical deposition [30, 31, 34, 35]. Indeed, an electrodeposition model proposed in Ref. [36] has

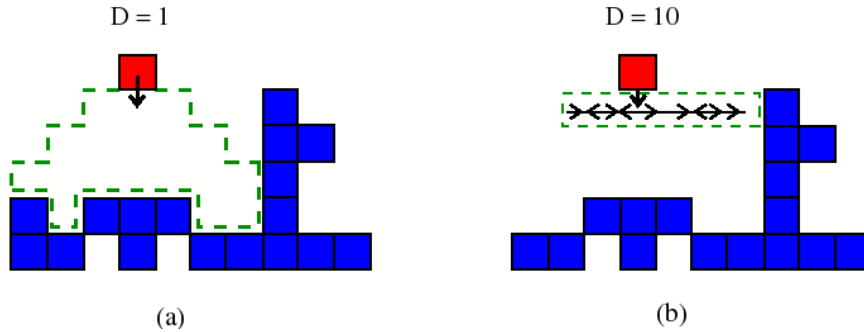


Figure 1. (Color online) Flow of a (red) particle towards the (blue) deposit with (a) $D = 1$ and (b) $D = 10$. The region that the particle in (a) can reach after several vertical and horizontal steps is surrounded by the (green) dashed line, showing that aggregation will occur at the valley of the deposit. The region scanned by the particle in (b) after a single vertical step is also surrounded, which leads to aggregation to the protruding part of the deposit.

stochastic rules similar to the present model. Particle diffusion facilitates the aggregation at the protuberant parts of the deposit, thus representing the attraction of particles to those regions. On the other hand, the directed particle flux is characteristic of ballistic deposition (BD) [37, 1] (the RCA model interpolates BD for $D = 0$ and DLA for $D \rightarrow \infty$).

Figs. 1a and 1b illustrate the consequence of the horizontal diffusive motion when a particle incide near a protruding part of a deposit. For small D (Fig. 1a), the incoming particle is not able to stick to that surface feature because it rapidly flows towards the substrate. However, for large D (Fig. 1b), it samples a wide horizontal region after each vertical step, thus it is possible to attach to the protruding point.

In the colloidal particle deposition of Ref.[22], an attraction of elongated (large aspect ratio ϵ) particles to the protruding points of the deposit is observed. This is confirmed by the preferential sticking to the hills of the slightly rough contact line in the initial steps of the deposition [26]. For this reason, the application of our model to that problem requires larger values of D to be associated to larger values of ϵ . In this case, D should not be interpreted as a diffusion coefficient in solution. Instead, the scanned length proportional to $D^{1/2}$ (Fig. 1b) may be related to the range of the attractive particle-deposit interaction.

Simulations of the model were performed for several values of D between $D = 0$ (BD) and $D = 8$, in a substrate with 4096 sites, which is sufficiently large to avoid finite-size effects. The time unit is set as that necessary for the deposition of one layer of particles (4096 particles); since the deposits are porous, the average thickness after one time unit exceeds the particle size d .

The global roughness of the surface of a deposit at time t is defined as the rms fluctuation of the height h around its average position \bar{h} :

$$w(t) \equiv \left\langle \overline{(h - \bar{h})^2}^{1/2} \right\rangle, \quad (1)$$

where the overbars indicate spatial averages and the angular brackets indicate configurational averages. The local roughness $w_{loc}(l, t)$ is defined as the rms height fluctuation averaged inside a box of linear size l that slides along the surface, parallel to the substrate.

The autocorrelation function is defined as

$$\Gamma(r, t) \equiv \langle \tilde{h}(x, t) \tilde{h}(x + r, t) \rangle, \quad (2)$$

where $\tilde{h} \equiv h - \bar{h}$ and the brackets represent an average over different positions x along the substrate.

In sufficiently large substrates (in which finite-size effects are negligible), the global roughness scales as

$$w \sim t^\beta, \quad (3)$$

where β is called roughness exponent. For box sizes smaller than the lateral correlation length, the local roughness of a system with normal scaling depends on l as

$$w_{loc} \sim l^\alpha, \quad (4)$$

where α is the roughness exponent [in systems with anomalous scaling [38], α is replaced by the local roughness exponent in Eq. (4), which differs from the global roughness exponent].

The first zero (r_0) or the first minimum (r_m) of the autocorrelation function $\Gamma(r, t)$ gives an estimate of the lateral correlation length of the surface at time t . They are expected to scale as

$$r_0, r_m \sim t^{1/z}, \quad (5)$$

where $z = \alpha/\beta$ is the dynamic exponent.

Since the colloidal particle deposition of Ref.[22] is a motivation for this study, it is important to account for the order of magnitude of the quantities involved there. The average diameter of spherical particles is $\langle d \rangle = 1.3\mu m$, and elongated particles have similar characteristic size. The maximal average height of the deposits is near $30\mu m$, which amounts to $23\langle d \rangle$. This justifies the study of short time features of the model, since that thickness corresponds to deposition of nearly 23 complete layers in a compact film, but much less in a porous film.

A more subtle point is that the roughness exponent was measured in box sizes ranging from $l_{min} \approx 0.1\mu m$ to $l_{max} \approx 10\mu m$ in Ref.[22], (the local roughness is measured until saturation, in sizes up to $l \approx 200\mu m$ or $300\mu m$). These sizes range from $l_{min} \approx 0.08d$ to $l_{max} \approx 8d$, thus the scaling exponents are probing height fluctuations inside a single particle (intra-particle features) as well as height fluctuations of sets with several particles. This justifies the use of models describing intra-particle features along the lines of Refs. [39, 29].

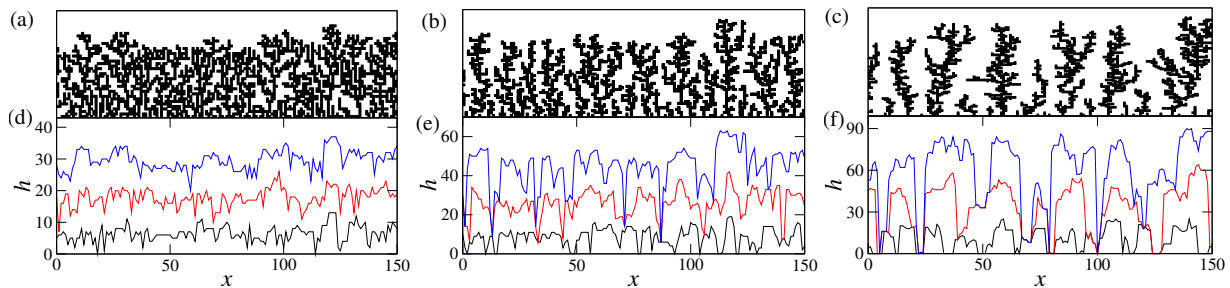


Figure 2. (Color online) Typical deposits (top) and height profiles (bottom) of the RCA model after deposition of 4 (black), 10 (red), and 16 (blue) particle layers, for: (a) $D = 0$, (b) $D = 2$, and (c) $D = 8$. h and x are measured in units of the particle size d .

3. Interface profiles and growth exponents

Figs. 2a-c show sections of the deposits generated by the model with $D = 0$ (BD), $D = 2$, and $D = 8$, after deposition of 16 layers of particles. The increase of D is responsible for the decrease of the film density, as observed in Ref. [27]. For this reason, the same deposition time leads to very different average heights, which range from $30d$ to $61d$ in Figs. 2a-c. Figs. 2d-f show the interface profiles at three different times for the same values of D of Figs. 2a-c (the interfaces for the longest time correspond to the deposits shown in Figs. 2a-c). The interface height at each column x [$h(x)$] is defined as the largest y value of an aggregated particle at x .

The branched structure shown in Figs. 2a-c is similar to that obtained in the RCA model [27]. However, a surprising result is the combination of this branched structure of the deposits and the columnar structure of the corresponding interface profiles (Figs. 2d-f), which parallel the features of colloidal particle deposits of Ref. [22] with large ϵ .

For large D , those columnar structures persist up to relatively long times. For this reason, a long crossover to KPZ scaling is expected with large D . Surfaces with columnar features are characteristic of processes in which the local growth rate is spatially inhomogeneous (larger at the hills, smaller at the valleys), in contrast with the translational symmetry of the KPZ and similar stochastic equations [1]. With columnar structures, the height fluctuations between hills and valleys increase linearly in time, thus a growth exponent [Eq. 3] near 1 is expected.

Fig. 3 shows the global roughness of the RCA films as a function of the average height for several values of D . The average height is nearly proportional to the deposition time t , but it is a more interesting quantity for comparison with experiments. The roughness clearly increases with D for deposits with the same thickness, in agreement with previous results [27].

For $D = 0$, a short time crossover is clear from the downward curvature of the $\log w \times \log \langle h \rangle$ plot, thus the estimate of β is highly dependent on the range of $\langle h \rangle$ chosen to fit. For example, for $2 \lesssim \langle h \rangle / d \lesssim 30$, we found local slopes continuously decreasing from 0.39 to 0.27. This range is used to determine the error bar in the

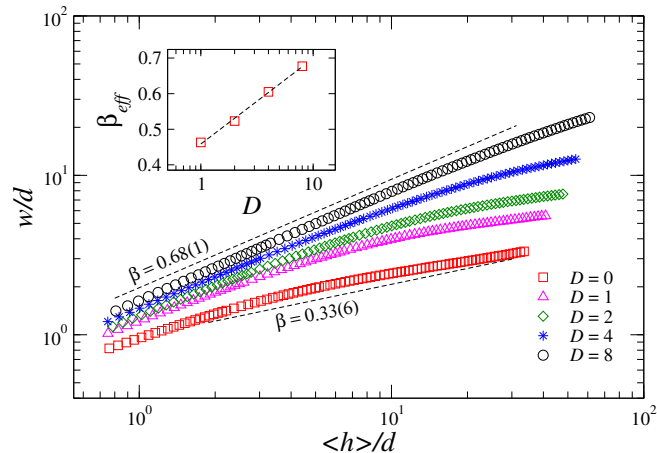


Figure 3. (Color online) Interface width w versus average height $\langle h \rangle$, rescaled by the particle size d , for the RCA model with several values of D . Dashed lines have the slopes indicated in the plot. The inset shows the effective growth exponents as a function of D .

estimate of β . The average slope is very close to the KPZ exponent $\beta_{KPZ} = 1/3$ [3], as shown in Fig. 3. However, BD is known to have a long crossover to KPZ scaling, so that deviations to smaller values of β are expected for slightly longer times, as shown in Ref. [40] and observed here.

For large D , reasonable linear fits can be obtained in almost two orders of magnitude of $\langle h \rangle$, as illustrated in Fig. 3. For $D = 8$, the growth exponent $\beta \approx 0.68$ is measured in that region and is much larger than the values of KPZ ($\beta = 1/3$) and of uncorrelated deposition ($\beta = 0.5$). This is consistent with the columnar growth illustrated in Fig. 2f. Thus, in applications with small film thicknesses, the scaling of the surface roughness may provide misleading information on the universality class of the growing system.

Fig. 3 considers thicknesses ranging from submonolayer coverage ($\langle h \rangle < d$) to some tens of the particle size, which is suitable for comparison with Ref. [22]. The exponents β at short times are in good agreement with those of the colloidal particle deposition of Yunker et al [22] for slightly anisotropic particles ($\epsilon = 1.2$, $\beta \approx 0.37$) and for highly anisotropic ones ($\epsilon = 3.5$, $\beta \approx 0.68$). However, the values of β for the model vary continuously between these limits as D increases, which differs from the apparent jumps in the experimental values of β (although the existence of a continuous but rapid change in the experimental exponents cannot be discarded).

A simple relation between the effective growth exponent and D can be derived with scaling arguments, as follows. For very short times, $w/d \approx 1$ and weakly depends on D , since submonolayer growth dominates, with rare aggregation at the second or third layers. However, for large thicknesses (e. g. $\langle h \rangle/d \sim 10^2$), the lateral diffusion length of incident particles is $l_{\parallel} \sim D^{1/2}$ for a small number of vertical steps, which leads to formation of valleys between the columns (Fig. 2f). The roughness is proportional to the height difference between those valleys and columns, which is expected to scale as l_{\parallel}^x , where $x > 0$ is some effective exponent (we are not attempted to assume that this is

the KPZ roughness exponent because this is a transient regime without KPZ scaling). This leads to $w/d \sim D^{x/2}$. The corresponding slope of the $\log w \times \log \langle h \rangle$ is of the form

$$\beta_{eff} \approx a + b \log D. \quad (6)$$

This is confirmed in the inset of Fig. 3, with $a \approx 0.4$ and $b \approx 0.1$.

Note that $\log D$ rapidly changes for small D , which leads to significant changes of the growth exponent shown in Fig. 3. The same rapid change occurs in $\log l_{\parallel}$. This means that small changes in the range of the attractive particle-deposit interaction may lead to large changes in the growth exponent. Indeed, transient scaling may be quite sensitive to details of the interactions, even if asymptotic scaling is the same.

A point that deserves particular attention in the colloidal particle deposition experiment is the estimate $\beta \approx 0.48$ for spherical particles ($\epsilon = 1$), which was interpreted as a consequence of uncorrelated random deposition in Ref. [22] (a model in which $\beta = 1/2$ [1]). However, the corresponding $\log w \times \log \langle h \rangle$ plot had a large number of data points with average height below $1.3\mu m$ and global roughness smaller than $0.7\mu m$ (in contrast to the fits of $\log w \times \log \langle h \rangle$ plots for other particle shapes, which have most data points with $\langle h \rangle > 1.3\mu m$). In the absence of discontinuities in that plot, those average heights may be representative of the early submonolayer regime, in which the roughness scales similarly to uncorrelated deposition.

Simulations of our model with $\langle h \rangle < d$ help to understand what is expected if submonolayer data is included in the calculation of the effective exponent β from $\log w \times \log \langle h \rangle$ plots. For small D , the submonolayer data gives slopes much larger than the slopes for $\langle h \rangle > d$, revealing a crossover which may eventually parallel the experiments with spherical particles. On the other hand, for large D , the slope with $\langle h \rangle < d$ is approximately the same measured with $\langle h \rangle > d$. Anyway, performing fits of the experimental data restricted to $\langle h \rangle > 1.3\mu m$ would be necessary to confirm these proposals.

4. Dynamic exponents

Broad ranges of dynamic exponents are also obtained for the short-time RCA model using the autocorrelation function.

Figs. 4a and 4b show the normalized autocorrelation function as a function of the distance r for $D = 0$ and $D = 8$, respectively, considering various average thicknesses. For $D = 0$, the minimum r_m of $\Gamma(r, t)$ is difficult to be identified, thus estimates of z are calculated only from the scaling of r_0 . For large values of D , $\Gamma(r, t)$ has a oscillatory structure with a clear minimum (Fig. 4b), which is a consequence of the columnar interface morphology (see also Ref. [41]).

The insets of Figs. 4a and 4b show the scaling of r_0 and r_m for $D = 0$ and $D = 8$, respectively. The estimates of the dynamic exponent are $z = 1.56 \pm 0.07$ and $z = 2.56 \pm 0.06$, respectively. The first estimate agrees with the KPZ value 1.5, but the second one is very far from that value. Again, a failure of KPZ scaling is observed for short growth times and for large lateral mobility of incident particles (large D).

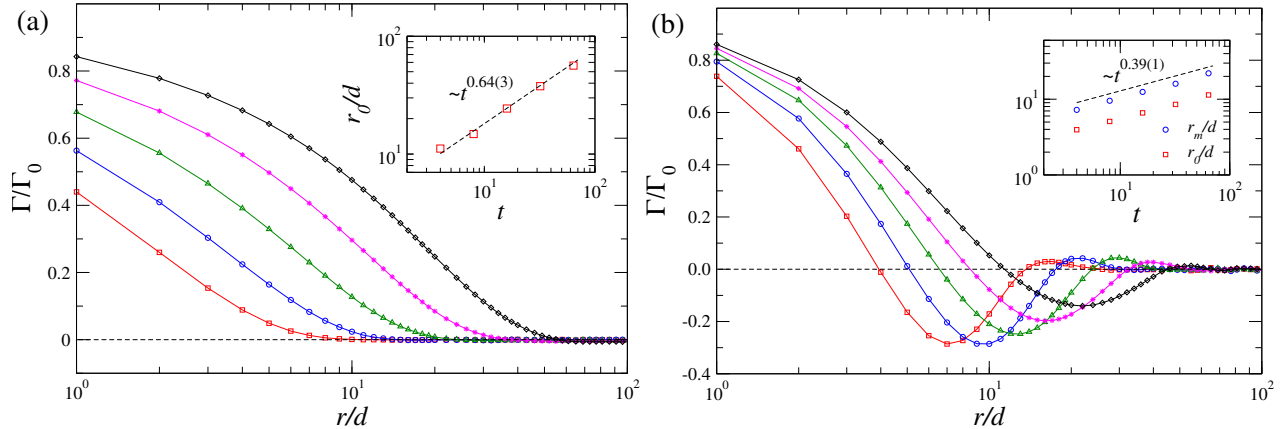


Figure 4. (Color online) Normalized autocorrelation function $\Gamma(r)/\Gamma(0)$ versus box size r rescaled by the particle size d , for (a) $D = 0$ and (b) $D = 8$, at deposition times $t = 4$ (red squares), 8 (blue circles), 16 (green triangles), 32 (magenta stars), and 64 (black diamonds). Times are measured in number of deposited monolayers.

The large effective dynamic exponent obtained for $D = 8$, as a consequence of the columnar morphology, is very different from the dynamic exponent $z = 1$ of QKPZ scaling. Thus, the particular features of the plots of the autocorrelation function and the estimates of dynamic exponents strongly suggest that these quantities should be studied in the colloidal particle deposits of Yunker et al [22] and related applications in order to understand their growth dynamics.

Comparison of Figs. 4a and 4b also shows that the apparent correlation length is much larger for $D = 0$ (BD). This occurs because the columnar structure for large D has lateral fluctuations determined by that parameter (as $l_{\parallel} \sim D^{1/2}$), which is not a KPZ feature. On the other hand, for $D = 0$, the fluctuations are determined by lateral propagation of correlations of KPZ type. Due to this complex interplay of lateral correlation mechanisms, no simple relation between the effective dynamical exponent z and the parameter D can be found, in contrast to that for the growth exponent [Eq. (6)].

5. Roughness exponents

In order to study the scaling of the local roughness, we will consider the models proposed in Ref. [29] to account for the shape of the aggregated particles.

After the deposits are grown, each deposited particle is transformed in a square of lateral size Sd , with integer $S > 1$. Then, a semiellipsoid of horizontal size Sd and height Hd is placed on the top of each surface square, as illustrated in the inset of Fig. 5. Here, we consider $S = 16$ and values of H ranging from 8 (circles) to 28 (semiellipsoids with aspect ratio 3.5).

Fig. 5 shows the local roughness as a function of the box size for two extremal values of D (0 and 8) and H (8 and 28).

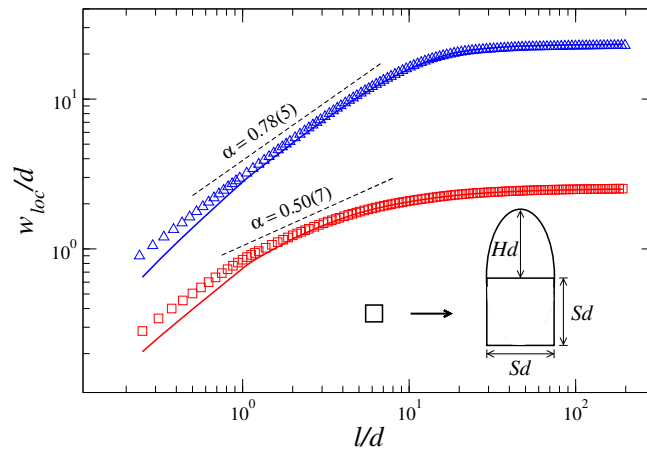


Figure 5. (Color online) Local roughness w_{loc} versus the box size l , rescaled by the particle size d , for $D = 0$ and $H = 8$ (red full line), $D = 0$ and $H = 28$ (red squares), $D = 8$ and $H = 8$ (blue full line) and $D = 8$ and $H = 28$ (blue triangles). Dashed lines have the slopes indicated in the plot. The inset illustrates the model of interface particles with ellipsoidal shape.

For $H = 8$ (circles), a crossover is observed as l crosses the particle size d for both values of D . For $D = 0$, the initial slope is slightly larger than the KPZ one, $\alpha = 0.5$, and evolves to values below that one, until saturating. The slope indicated in Fig. 5 represents the extremal values in the range $1 \lesssim l/d \lesssim 10$. For $D = 8$, the crossover is less salient, but the slopes are very different from the KPZ one; they range from ~ 1 for $l < d$ to ≈ 0.78 for $l > d$, far from saturation. The results for $H = 28$ (thinnest semiellipsoids) show a smooth crossover effect for $D = 0$ and a negligible one for $D = 8$. In the last case, a slope $0.78(5)$ is obtained in almost two decades of l , as illustrated in Fig. 5.

The value of D determines the order of magnitude of the roughness in each box size l , as shown by the large distance of the curves for $D = 0$ and $D = 8$ in Fig. 5. This is a consequence of the columnar structure, which increases the value of the roughness by a factor of order $D^{x/2}$, as explained in Sec. 3. The value of D also determines the scaling for $l > d$, with larger D giving larger effective roughness exponents.

On the other hand, the initial slope ($l < d$) is determined by the particle shape, i. e., by the value of H , as discussed in Ref. [29]. Increasing H corresponds to adding a larger constant term to the roughness, which is related to the intrinsic width [39]. This leads to a decrease of the initial slope.

The presence of a crossover or of a smooth scaling in the $\log w_{loc} \times \log l$ depends on the combination of these effects. As illustrated in Fig. 5, the particular case $D = 8$, $H = 28$, leads to apparently smooth scaling with an exponent much larger than the KPZ value. Due to this complex interplay of short range and long range effects, we are not able to derive a simple relation between the effective roughness exponent and the parameters D and H . However, the trend in all cases is that effective exponents exceed the KPZ value.

In colloidal particle deposits of Yunker et al [22], the roughness exponents range from 0.51(5) for spherical particles to 0.61(2) for the most elongated particles. The exponents obtained in our model span a much larger range, possibly because all deposited particles were stretched in the vertical direction and this stretching leads to a nontrivial change in the scaling (e. g. adding a constant term instead of a multiplicative factor). However, the trend of the roughness exponent increasing with ϵ in that experiment parallels the trend of increase with D in our model.

It is also important to observe that our exponent estimates for $D = 8$ do not obey the scaling relation $z = \alpha/\beta$. However, we stress that they are effective exponents obtained in a transient regime, with very small film thicknesses, and are different from the asymptotic (KPZ) exponent values that do obey that relation.

6. Asymptotic scaling

The RCA model was shown to belong to the KPZ class in 2+1 dimensions [27]. However, as far as we know, no previous work has studied the scaling of that model in 1 + 1 dimensions. For this reason, this section is devoted to the study of the asymptotic class of our deposition model (which is an extension of the RCA model) in 1 + 1 dimensions.

Fig. 6a shows the time evolution of the global roughness w for the model with $D = 4$ in a substrate of size $L = 4096$. The maximal time is chosen very far from the saturation regime. An initial rapid increase of w is observed, with slope near 0.61, which is related to the formation of the columnar structure. Subsequently, w slowly increases, with slope near 0.15 in Fig. 6a. However, this slope is continuously increasing and attains a value near 0.23 for $\langle h \rangle / d > 5000$. These features show that a long crossover is present in the model. This is not unexpected in a ballistic-like model; indeed, large scale simulations of BD and related models are necessary to provide asymptotic KPZ exponents with good accuracy [42].

Based on the experience with other ballistic-like models, we assume that the square roughness has the expected asymptotic form proportional to $t^{2\beta}$ with a constant correction term w_I^2 , which is usually called intrinsic width [43, 44]. Since estimating this term is typically difficult, our procedure is to analyze the relation between $w^2(t) - w^2(t_0)$ and $t - t_0$, with a suitable choice of t_0 . Inspection of 6a suggests using $t_0 = 40$, in which $w^2(t_0) = 378.6$, since this time slightly exceeds the transient region. Fig. 6b shows $\log [w^2(t) - w^2(t_0)]$ versus $\log(t - t_0)$, which gives $2\beta \approx 0.63$ in two decades of the variable t , in good agreement with the KPZ value $2\beta = 2/3$.

Additional support for the KPZ scaling is provided by calculation of saturation times of smaller systems, with sizes between $L = 64$ and $L = 1024$. Estimating the saturation time from the convergence of the roughness to the saturation value is a difficult task. However, an alternative is suggested in Ref. [45] and is extended here to cases with large intrinsic roughness, as follows.

The Family-Vicsek (FV) scaling relation [46] [which contains the relations (3) and (4) as limiting cases] can be written as $w^2(t, L) = w_{sat}^2 f(t/L^z)$, where f is a scaling

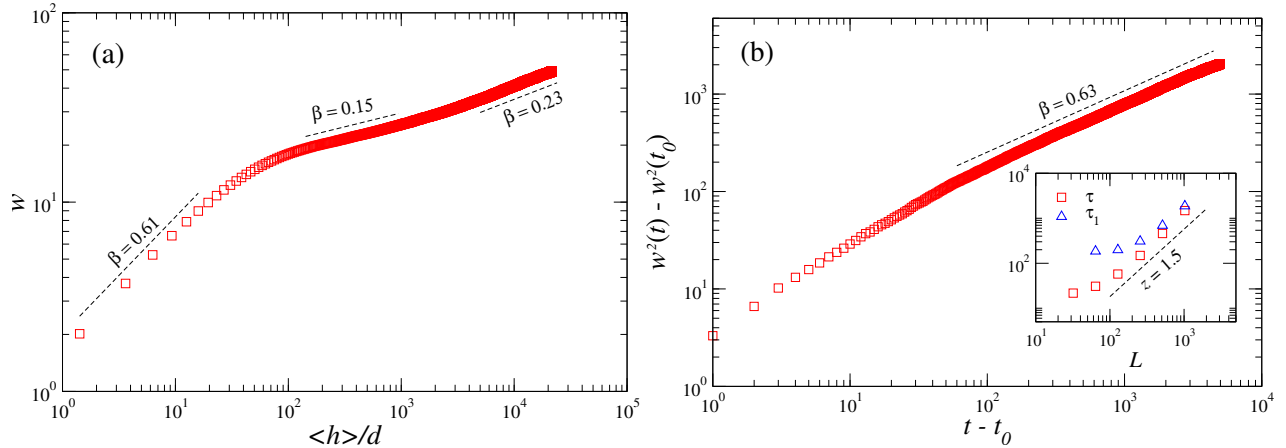


Figure 6. (Color online) a) Roughness evolution in time, for $D = 4$ and long growth times. b) Reduced square roughness $w^2(t) - w^2(t_0)$ versus reduced time $t - t_0$, for the same data of (a). Inset shows the characteristic saturation times τ and τ_1 against the substrate size L .

function so that $f(x) \rightarrow 1$ as $x \rightarrow \infty$ and $f(x) \sim x^\beta$ for $x \ll 1$. The characteristic time τ is defined as $w^2(\tau) = kw^2_{sat}$, for fixed L and fixed $k < 1$. Using the FV relation, we have $\tau \sim L^z$ [45]. In the presence of an intrinsic roughness $w^2(t_0)$, the FV relation may be written as $w^2(t, L) - w^2(t_0) = [w^2_{sat} - w^2(t_0)]g[(t - t_0)/\tau]$, where the function g has the same asymptotic forms of f . Thus, a characteristic time τ_1 is defined as $w^2(\tau_1) - w^2(t_0) = k[w^2_{sat} - w^2(t_0)]$, for fixed L and fixed $k < 1$. For long times, it gives $\tau_1 \sim L^z$.

In the inset of Fig. 6b we show τ and τ_1 as a function of the lattice size L . For small L , a slow increase of those characteristic times is observed. However, the largest values of L suggest a convergence to the KPZ scaling with slope $3/2$. The usual method of calculating effective exponents from the data in sizes L and $L/2$ is not helpful in this case because only the last three data points belong to a scaling region.

7. Discussion and conclusion

We performed a detailed analysis of the short time scaling of height fluctuations of a model [27], which mimics the ‘‘Matthew effect’’ recently observed in colloidal particle deposition at the edges of evaporating drops [22]. Increasing the number of horizontal random steps D in the model is equivalent to increasing the range of attraction between deposited and wandering particles and leads to increasing effective growth exponents, ranging from $\beta \approx 0.33$ to $\beta \approx 0.68$, in good agreement with the experimental estimates. The local roughness was measured accounting for intra-particle scales and provided a broad range of roughness exponents, also including the estimates of that colloidal particle deposition. Notwithstanding, the morphology of deposits and height profiles obtained with the model are similar to the ones shown in Ref. [22].

The large growth and roughness exponents observed here for large D are simple

consequences of the initial columnar growth present in the system. Since this columnar growth is also observed in the experiments with highly elongated particles ϵ [22], there is no need to invoke a critical KPZ dynamics with quenched disorder to explain those features, as previously pointed out by Nicoli et al. [25]. After this *transient* columnar growth, our model suggests that a crossover to universal KPZ scaling is possible.

In order to decide between these different interpretations, we propose to measure the dynamic exponent z from the first zero or minima of the autocorrelation function. For small D , this function have the behavior expected for self-affine interfaces and the corresponding dynamic exponent agrees with the KPZ value $z = 1.5$. However, for large D , the autocorrelation function has an oscillatory behavior due to the columnar structures and provides much larger estimates of z (far from the QKPZ value $z \approx 1$). This proposal may also be very important for future works to decide between a true dynamic scaling and possible transient behaviors, particularly because the scaling law $z = \alpha/\beta$ does not hold for the latter.

Acknowledgments

The authors thank R. Cuerno for helpful discussions. This work was supported by FAPEMIG, FAPERJ, and CNPq (Brazilian agencies).

References

- [1] Barabási A and Stanley H 1995 *Fractal concepts in surface growth* (Cambridge, England: Cambridge University Press)
- [2] Ohring M *Materials Science of Thin Films - Deposition and Structure* 2nd ed (California, USA: Academic Press)
- [3] Kardar M, Parisi G and Zhang Y C 1986 *Phys. Rev. Lett.* **56** 889
- [4] Sasamoto T and Spohn H 2010 *Phys. Rev. Lett.* **104** 230602
- [5] Amir G, Corwin I and Quastel J 2011 *Commun. Pure Appl. Math.* **64** 466
- [6] Calabrese P and Doussal P L 2011 *Phys. Rev. Lett.* **106** 250603
- [7] Imamura T and Sasamoto T 2012 *Phys. Rev. Lett.* **108** 190603
- [8] Ebothé J, Hichou A E, Vautrot P and Addou M 2003 *J. Appl. Phys.* **93** 632
- [9] Kleinke M U, Davalos J, da Fonseca C P and Gorenstein A 1999 *Appl. Phys. Lett.* **74** 1683
- [10] de Souza N C, Ferreira M, Wohnrath K, Silva J R, Oliveira Jr O N and Giacometti J A 2007 *Nanotechnology* **18** 075713
- [11] Ferreira S O, Ribeiro I R B, Suela J, Menezes-Sobrinho I L, Ferreira S C and Alves S G 2006 *Appl. Phys. Lett.* **88** 244102
- [12] Huo S and Schwarzacher W 2001 *Phys. Rev. Lett.* **86** 256
- [13] Lafouresse M C, Heard P J and Schwarzacher W 2007 *Phys. Rev. Lett.* **98** 236101
- [14] Placidi E, Arciprete F, Balzarotti A and Patella F 2012 *Appl. Phys. Lett.* **101** 141901
- [15] Majaniemi S, Ala-Nissila T and Krug J 1996 *Phys. Rev. B* **53** 8071
- [16] Krug J and Rost M 1999 *Phys. Rev. B* **60** R16334
- [17] Grossmann B, Guo H and Grant M 1991 *Phys. Rev. A* **43** 1727
- [18] Nattermann T and Tang L H 1992 *Phys. Rev. A* **45** 7156
- [19] Oliveira T J, Dechoum K, Redinz J A and Aarão Reis F D A 2006 *Phys. Rev. E* **74** 011604
- [20] Aarão Reis F D A 2006 *Phys. Rev. E* **73** 021605
- [21] Horowitz C M and Albano E V 2006 *Phys. Rev. E* **73** 031111

- [22] Yunker P J, Lohr M A, Still T, Borodin A, Durian D J and Yodh A G 2013 *Phys. Rev. Lett.* **110** 035501
- [23] Csahok Z, Honda K and Vicsek T 1993 *J. Phys. A* **26** L171
- [24] Merton R K 1968 *Science* **159** 56
- [25] Nicoli M, Cuerno R and Castro M 2013 *Phys. Rev. Lett.* **111** 209601
- [26] Yunker P J, Lohr M A, Still T, Borodin A, Durian D J and Yodh A G 2013 *Phys. Rev. Lett.* **111** 209602
- [27] Rodríguez-Pérez D, Castillo J L and Antoranz J C 2005 *Phys. Rev. E* **72** 021403
- [28] Rodríguez-Pérez D, Castillo J L and Antoranz J C 2007 *Phys. Rev. E* **76** 011407
- [29] Oliveira T J and Aarão Reis F D A 2011 *Phys. Rev. E* **83** 041608
- [30] Castro M, Cuerno R, Sánchez A and Domínguez-Adame F 1998 *Phys. Rev. E* **57** R2491
- [31] Castro M, Cuerno R, Sánchez A and Domínguez-Adame F 2000 *Phys. Rev. E* **62** 161
- [32] Galindo J L and Huertas R 2013 *J. Appl. Phys.* **114** 064905
- [33] Witten T A and Sander L M 1981 *Phys. Rev. Lett.* **47** 1400
- [34] Ferreira S C, Alves S G, Brito A F and Moreira J G 2005 *Phys. Rev. E* **71** 051402
- [35] Nicoli M, Castro M and Cuerno R 2009 *J. Stat. Mech.* **2009** P02036
- [36] Hill S C and Alexander J I D 1997 *Phys. Rev. E* **56** 4317
- [37] Vold M J 1959 *J. Phys. Chem.* **63** 1608
- [38] Ramasco J J, López J M and Rodríguez M A 2000 *Phys. Rev. Lett.* **84** 2199
- [39] Oliveira T J and Aarão Reis F D A 2007 *J. Appl. Phys.* **101** 063507
- [40] Aarão Reis F D A 2001 *Phys. Rev. E* **63** 056116
- [41] Siniscalco D, Edely M, Bardeau J F and Delorme N 2013 *Langmuir* **29** 717
- [42] Farnudi B and Vvedensky D D 2011 *Phys. Rev. E* **83** 020103(R)
- [43] Zabolitzky J G and Stauffer D 1986 *Phys. Rev. A* **34** 1523
- [44] Kertész J and Wolf D E 1988 *J. Phys. A* **21** 747
- [45] Aarão Reis F D A 2002 *Physica A* **316** 250
- [46] Family F and Vicsek T 1985 *J. Phys. A* **18** L75